U-Load Dextramer®
Build multimers with your choice of peptide and peptide-receptive MHC I and MHC II alleles.

The Journal of Immunology

This information is current as of February 24, 2022.

Evaluation of Cellular and Serological Responses to Acute SARS-CoV-2 Infection Demonstrates the Functional Importance of the Receptor-Binding Domain

Grace Mantus, Lindsay E. Nyhoff, Robert C. Kauffman, Venkata Viswanadh Edara, Lilin Lai, Katharine Floyd, Pei-Yong Shi, Vineet D. Menachery, Srilatha Edupuganti, Erin M. Scherer, Ariel Kay, Nina McNair, Evan J. Anderson, Nadine Rouphael, Rafi Ahmed, Mehul S. Suthar and Jens Wrammert

J Immunol 2021; 206:2605-2613; Prepublished online 5 May 2021;
doi: 10.4049/jimmunol.2001420
http://www.jimmunol.org/content/206/11/2605

Supplementary Material **http://www.jimmunol.org/content/suppl/2021/05/05/jimmunol.2001420.DCSupplemental**

References This article **cites 38 articles**, 5 of which you can access for free at:
http://www.jimmunol.org/content/206/11/2605.full#ref-list-1

Why *The JI*? Submit online.

- **Rapid Reviews! 30 days*** from submission to initial decision
- **No Triage!** Every submission reviewed by practicing scientists
- **Fast Publication!** 4 weeks from acceptance to publication

**average*

Subscription Information about subscribing to *The Journal of Immunology* is online at:
http://jimmunol.org/subscription

Permissions Submit copyright permission requests at:
http://www.aai.org/About/Publications/JI/copyright.html

Email Alerts Receive free email-alerts when new articles cite this article. Sign up at:
http://jimmunol.org/alerts

The Journal of Immunology is published twice each month by
The American Association of Immunologists, Inc.,
1451 Rockville Pike, Suite 650, Rockville, MD 20852
Copyright © 2021 by The American Association of Immunologists, Inc. All rights reserved.
Print ISSN: 0022-1767 Online ISSN: 1550-6606.

Downloaded from http://www.jimmunol.org/ by guest on February 24, 2022

Evaluation of Cellular and Serological Responses to Acute SARS-CoV-2 Infection Demonstrates the Functional Importance of the Receptor-Binding Domain

Grace Mantus,*,†,1 Lindsay E. Nyhoff,*,†,1 Robert C. Kauffman,*,†,1 Venkata Viswanadh Edara,†,‡,§ Lilin Lai,†,‡,§ Katharine Floyd,†,‡,§ Pei-Yong Shi,¶ Vineet D. Menachery,‖ Srilatha Edupuganti,# Erin M. Scherer,# Ariel Kay,# Nina McNair,# Evan J. Anderson,* Nadine Rouphael,# Rafi Ahmed,†, Mehul S. Suthar,*,†,‡ and Jens Wrammert*,†**

The factors that control the development of an effective immune response to the recently emerged SARS-CoV-2 virus are poorly understood. In this study, we provide a cross-sectional analysis of the dynamics of B cell responses to SARS-CoV-2 infection in hospitalized COVID-19 patients. We observe changes in B cell subsets consistent with a robust humoral immune response, including significant expansion of plasmablasts and activated receptor-binding domain (RBD)–specific memory B cell populations. We observe elevated titers of Abs to SARS-CoV-2 RBD, full-length Spike, and nucleoprotein over the course of infection, with higher levels of RBD-specific IgG correlating with increased serum neutralization. Depletion of RBD-specific Abs from serum removed a major portion of neutralizing activity in most individuals. Some donors did retain significant residual neutralization activity, suggesting a potential Ab subset targeting non-RBD epitopes. Taken together, these findings are instructive for future vaccine design and mAb strategies. *The Journal of Immunology*, **2021, 206: 2605–2613.**

The novel coronavirus, SARS-CoV-2, emerged in December 2019 (1) and continues to take an unprecedented toll on the global population, with over 2.4 million deaths reported worldwide, a half million of which have occurred in the United States alone (2). Two mRNA vaccines (Pfizer-BioNTech and Moderna) are currently approved for emergency use in the U.S. (3, 4). In addition to these U.S.–approved SARS-CoV-2 vaccines, there are over 200 other vaccine candidates at various developmental stages, from preclinical testing to approved usage outside the U.S. (5). To understand the differences in efficacy between vaccine candidates and between immunity developed from vaccination versus natural infection, it is important to continue to explore the characteristics of protective immunity after natural infection. Discoveries concerning the generation, dynamics, and durability of natural immunity may influence discussions and decisions concerning future vaccination development and distribution efforts. Furthermore, a detailed insight into the mechanism of viral neutralization is also essential for both vaccine and mAb-based treatment efforts, potentially influencing considerations of necessary Ag targets to achieve effective thresholds of protection.

SARS-CoV-2, a β-coronavirus (6), shares a high level of homology to SARS-CoV (1), the coronavirus responsible for the 2002–2003 SARS epidemic. These coronaviruses have also been found to share the same host entry receptor, ACE2, which is bound by the receptor-binding domain (RBD) on the Spike (S) homotrimer that is present on the viral surface (7). RBD is located within the S1

*Centers for Childhood Infections and Vaccines, Children's Healthcare of Atlanta and Emory University, Department of Pediatrics, Atlanta, GA; †Emory Vaccine Center, Emory University School of Medicine, Atlanta, GA; ‡Division of Infectious Diseases, Department of Pediatrics, Emory University School of Medicine, Atlanta, GA; §Yerkes National Primate Research Center, Atlanta, GA; ¶Department of Microbiology and Immunology, Institute for Human Infection and Immunity, World Reference Center for Emerging Viruses and Arboviruses, University of Texas Medical Branch, Galveston, TX; ‖Department of Biochemistry and Molecular Biology, The University of Texas Medical Branch, Galveston, TX; #Hope Clinic of the Emory Vaccine Center, Division of Infectious Diseases, Department of Medicine, Emory University School of Medicine Decatur, Atlanta, GA; and **Department of Microbiology and Immunology, Emory University School of Medicine, Atlanta, GA 30322

[1]G.M., L.E.N., and R.C.K. contributed equally.

ORCIDs: 0000-0001-5767-6122 (L.E.N.); 0000-0001-9321-7839 (V.V.E.); 0000-0002-0866-6961 (K.F.); 0000-0002-8794-1932 (E.M.S.); 0000-0003-4338-7017 (A.K.), 0000-0002-1576-4420 (E.J.A.); 0000-0002-2686-8380 (M.S.S.).

Received for publication December 18, 2020. Accepted for publication March 18, 2021.

This work was supported in part by an Emory Executive Vice President for Health Affairs Synergy Fund award (to M.S.S. and J.W.), the Woodruff Health Sciences Center, which supplied COVID-Catalyst-I3 funds (to M.S.S.), the Center for Childhood Infections and Vaccines (to J.W. and M.S.S.), Children's Healthcare of Atlanta (to J.W. and M.S.S.), a Woodruff Health Sciences Center 2020 COVID-19 CURE Award (to M.S.S.), and by the National Institutes of Health, National Institute for Allergy and Infectious Diseases (NIH) under award numbers P51OD011132 (to M.S.S.) and 3U19AI057266-17S1 (to J.W., R.A., and M.S.S.), and the Infectious Diseases Clinical Research Consortium UM1AI148684 (to N.R., E.J.A., J.W., and M.S.S.), R00AG049092 (to V.D.M.), and the World Reference Center for Emerging Viruses and Arboviruses R24AI120942 (V.D.M.). The content is solely the responsibility of the authors and does not necessarily represent the official views of the NIH. The funders had no role in study design, data collection and analysis, decision to publish, or preparation of the manuscript.

Author contributions: G.M., L.E.N., and R.C.K. contributed to the acquisition, analysis, and interpretation of data and writing the manuscript. V.V.E., L.L., and K.F. performed in vitro neutralization experiments. P.-Y.S. and V.D.M. provided the viral clones used for in vitro neutralization assays. S.E. served as the principal investigator of the clinical protocol for acquisition of patient samples. E.M.S., A.K., and N.M. provided clinical support for the study and contributed to sample collection and analysis. E.J.A., N.R., R.A., M.S.S., and J.W. contributed to the conception and design of the work and the writing and approval of the final manuscript.

Address correspondence and reprint requests to Dr. Jens Wrammert, Emory Children's Center, Department of Pediatrics, Emory University, 2015 Uppergate Drive, Atlanta, GA 30329. E-mail address: jwramme@emory.edu

The online version of this article contains supplemental material.

Abbreviations used in this article: DPBS, Dulbecco PBS; DpSO, day postsymptom onset; FRNT, focus reduction neutralization titer; icSARS-CoV-2; infectious clone SARS-CoV-2; IRB, Institutional Review Board; MBC, memory B cell; NP, nucleoprotein; PFA, paraformaldehyde; RBD, receptor-binding domain; S, Spike.

Copyright © 2021 by The American Association of Immunologists, Inc. 0022-1767/21/$37.50

www.jimmunol.org/cgi/doi/10.4049/jimmunol.2001420

Downloaded from http://www.jimmunol.org/ by guest on February 24, 2022

subunit of the protein and appears to be only accessible in the "open" or "up" confirmation of the trimer (7). Given the homology between the two β-coronaviruses, a predictable relationship between RBD binding and SARS-CoV-2 neutralization exists, and studies by us (8) and others (9–11) have clearly illustrated a strong correlation between RBD binding and viral neutralization. Like their SARS-CoV counterparts, Abs targeting RBD appear to be an integral component of the protective immune response against SARS-CoV-2 (12). In support of this, several Abs isolated from RBD-specific memory B cells (MBCs) have been characterized and shown to be potent neutralizers of SARS-CoV-2, both in vitro (11, 13, 14) and in vivo (15). In addition, several groups have shown potent plasmablast responses during acute infection (16) and sizeable RBD- or S-specific MBC responses (11, 13–15, 17) early postinfection. Interestingly, potent RBD-specific neutralizing Abs can be isolated from individuals, regardless of the neutralizing serum titer (11), and follicular T cells, a critical part of germinal center reactions, are rarely RBD-specific (17). Given the contribution of Abs to the neutralization of SARS-CoV-2 in vivo, understanding the protective characteristics of the virus-specific B cell responses to SARS-CoV-2 infection remains crucial.

An early expansion of plasmablasts followed by the formation of a circulating Ag-specific MBC pool has been reported for numerous acute viral infections, including SARS-CoV-2 (11, 13–17). Previous studies of SARS-CoV and SARS-CoV-2 infection have shown that patients develop severe lymphopenia with significant decreases in T cell numbers. In contrast, B cell numbers in these individuals remain unimpacted by infection (18, 19). However, recent evidence from autopsied patients that succumbed to SARS-CoV-2 infection suggests suboptimal germinal center reactions in these patients, which could potentially contribute to short-lived and immature Ab responses to SARS-CoV-2 (16, 20). Additional alterations among B cell subsets have also been reported. For example, expanded atypical MBCs have been reported in patients with severe COVID-19 (20, 21). A subset most often described in patients with autoimmunity, immunodeficiencies, or chronic viral infection, these $CD27^{-}CD21^{-}$ B cells are thought to mature independently of germinal center reactions through an extrafollicular pathway (21, 22). The apparent expansion of this subset within patients with severe COVID-19 raises questions concerning the nature of their role in the immune response to SARS-CoV-2 and their contribution to durable Ab responses, which is a continued concern, given several recent reports of SARS-CoV-2 reinfection after only a few months in individuals previously infected with SARS-CoV-2 (23, 24).

In this study, we report a cross-sectional study of the dynamics of human B cell responses during acute SARS-CoV-2 infection. We show that infection induces both potent plasmablast and RBD-specific MBC responses that correlate with virus-specific serological responses. We also show, using a serum-depletion approach, that RBD-specific Abs are the primary driver of viral neutralization in the majority of patients. Interestingly, a subset of the individuals examined had significant portions of their neutralizing response that appeared resistant to RBD depletion, potentially suggesting alternate mechanisms of protection outside the direct inhibition of RBD. These findings have significant implications for ongoing vaccine strategies, as well as for efforts to identify, characterize, and deploy preventative and therapeutic mAbs against SARS-CoV-2.

Materials and Methods

Study cohort

The current study draws on patient samples from hospitalized COVID-19 patients with RT-PCR–confirmed SARS-CoV-2 infection at the Emory University Hospital and Emory University Hospital Midtown (n = 50). Although no specific criteria or demographics were used for enrollment beyond PCR-confirmed SARS-CoV-2 infection, all patients were symptomatic at the time of enrollment. Specimens were collected after receiving informed consent, except for 00022371, for which a consent waiver was obtained. The clinical studies from which these samples were obtained was approved by the Emory University Institutional Review Board (IRB) number 00000510, IRB number 00045690, and IRB number 0022371. For IRB numbers 00000510 and 00045690, informed consent was obtained prior to patient participation. For number 00022371, an IRB waiver was obtained, allowing the use of discarded samples in the clinical laboratory at the Emory Hospital. The majority of the patients were diagnosed with severe disease (91%) and trended toward being older (median age = 58.5) and male (59%). Further details of the cohort can be found in Supplemental Table I. Limitations of the cohort include the following: 1) all individuals were hospitalized with the majority diagnosed with severe disease, 2) a majority of individuals had one or more pre--existing conditions, and 3) a relatively small sample size.

Sample preparation

Briefly, plasma and PBMC were isolated from peripheral blood collected in CPT tubes from these patients at various times after disease onset (3–57 d after symptom onset). Briefly, CPT tubes were processed according to the manufacturer's protocol, and separated plasma and PBMCs were collected separately. PBMCs were treated with ACK lysis buffer (catalog no. 118-156-101, Quality Biological) for 5 min and washed three times with PBS with 2% FBS before counting and analysis by flow cytometry. PBMC and plasma were frozen at −80C prior to long-term storage at −80C (plasma) or in liquid nitrogen (PBMC).

Viruses and cells

The infectious clone SARS-CoV-2 (icSARS-CoV-2) and mNG-tagged SARS-CoV-2 (icSARS-CoV-2-mNG) were kindly provided to us and previously described by Dr. Vineet Menachery (University of Texas Medical Branch) (25). Briefly, the SARS-CoV-2 virus used was derived from infectious clone 2019-nCOV/USA_WA1/2020 and tagged with a fluorescent reporter gene (mNG) in ORF7 (25). Viral titers were determined by plaque assay on VeroE6 cells (American Type Culture Collection). VeroE6 cells were cultured in complete DMEM consisting of 1× DMEM (Corning Cellgro), 10% FBS, 25 mM HEPES buffer (Corning Cellgro), 2 mM L-glutamine, 1mM sodium pyruvate, 1× nonessential amino acids, and 1× antibiotics. Viral stocks were titrated on VeroE6 cells and stored at −80°C until use.

Flow cytometry

Freshly isolated PBMCs were stained first for viability with LIVE/DEAD Fixable Yellow (Thermo Fisher Scientific) and then for markers with the following mAbs: IgA (IS11-8E10; Miltenyi Biotec), IgD (IA6-2; BD Biosciences), IgG (G18-145; BD Biosciences), IgM (MHM-88; BioLegend), CD3 (SK7, BD Biosciences), CD4 (RPA-T4, BD Biosciences), CD8 (SK1; BD Biosciences), CD14 (61D3; eBioscience), CD16 (CB16; eBioscience), CD19 (SJ25C1; BD Biosciences), CD20 (2H7; BD Biosciences), CD27 (O323; BioLegend or M-T271; BD Biosciences), CD38 (HB7; BD Biosciences), and CD71 (CY1G4; BioLegend). Ag-specific B cells were detected by staining with RBD-conjugated to Alexa Fluor 488 (Alexa Fluor 488 Protein Labeling Kit; Thermo Fisher Scientific). RBD was conjugated according to the manufacturer's instructions, with the following changes: protein was labeled at a concentration of 1mg/ml and incubated for 30 min without the addition of bicarbonate. After staining, PBMCs were washed and then fixed for 30 min using 2% paraformaldehyde (PFA; Thermo Fisher Scientific). Data were acquired on a BD FACSymphony A5 and analyzed using FlowJo 10.7.1 (BD Biosciences).

ELISA

ELISAs were conducted as we have previously described (8). Recombinant RBD for this assay was generated as previously described (8). Briefly, recombinant RBD derived from SARS-CoV-2, Wuhan-Hu-1 (GenPept: QHD43416) was cloned, expressed in an Expi293F cell system, and purified on HisTALON Superflow Cartridges (8). Recombinant RBD, recombinant monomeric S (obtained from the Centers for Disease Control), or nucleoprotein (NP; catalog no. 40588-V08B; Sino Biological) were coated overnight at 4°C on MaxiSorp plates at 0.5 (NP) and 1 (RBD, S) μg/ml in Dulbecco PBS (DPBS). After blocking for 2 h with 1% BSA in PBS containing 0.05% Tween 20, serially diluted serum samples were added and incubated for 90 min. The bound Abs were detected using goat anti-human isotype-specific secondary Abs conjugated to HRP that were added for 60 min (anti-IgG, catalog no. 109-036-098; anti-IgM, catalog no. 109-036-129; anti-IgA, catalog no. 109-036-011; Jackson Immunoresearch Laboratories). Plates were developed with 0.4 mg/ml *o*-phenylenediamine dihydrochloride diluted in phosphate-citrate buffer (pH 5.0) containing 0.012% H_2O_2. The reaction was stopped with 1M hydrochloric acid, and the absorbance was measured

Downloaded from http://www.jimmunol.org/ by guest on February 24, 2022

at 490 nm using a spectrophotometer (Bio-Rad Laboratories). Unless noted, plates were washed three times with PBS containing 0.05% Tween 20 between each step. End-point titers were interpolated based on a sigmoidal four-parameter logistic, where X is concentration with the baseline value for each isotype/Ag pair derived from the average plus three times the SD of prepandemic negative control samples ($n = 20$).

Focus reduction neutralization titer assay

COVID-19 patient or healthy control plasma was incubated at 56°C for 30 min and manually diluted in duplicate in serum-free DMEM and incubated with 750–1000 focus-forming units of either icSARS-CoV-2 or SARS-CoV-2-mNG virus at 37°C for 1 h. The virus/serum mixture was added to VeroE6 cell monolayers seeded in 96-well clear or blackout plates and incubated at 37°C for 1 h. Postincubation, the inoculum was removed and replaced with prewarmed complete DMEM containing 0.85% methylcellulose. Plates were incubated at 37°C for 24 h. After 24 h, the methylcellulose overlay was removed, cells were washed three times with PBS, and fixed with 2% PFA in PBS for 30 min at room temperature. For the focus reduction neutralization titer (FRNT) assay, plates were washed twice with 1× PBS and 100 µl of permeabilization buffer (0.1% BSA–Saponin in PBS) (Sigma-Aldrich), was added to the fixated Vero cell monolayer for 20 min. Cells were incubated with an anti–SARS-CoV S protein primary Ab conjugated to biotin (CR3022–biotin) for 1 h at room temperature, then with avidin–HRP conjugated secondary Ab for 1 h at room temperature. Foci were visualized using TrueBlue HRP substrate and imaged on an ELISPOT reader (CTL Analyzers). For the FRNT-mNG assay, the 2% PFA is removed and washed twice with PBS. The foci were visualized using an ELISPOT reader (CTL ImmunoSpot S6 Universal Analyzer) under an FITC channel and enumerated using Viridot. The neutralization titers were calculated as follows: 1 − (ratio of the mean number of foci in the presence of sera and foci at the highest dilution of respective sera sample). Each specimen is tested in two independent assays performed at different times. The FRNT-mNG$_{50}$ titers were interpolated using a four-parameter nonlinear regression in GraphPad Prism 8.4.3. Samples with an FRNT$_{50}$ value that was below the limit of detection, are plotted at 10. For these samples, this value was used in fold reduction calculations.

Depletion of RBD-specific serum Ab

RBD binding Abs in patient sera were depleted using RBD-coupled paramagnetic beads. Recombinant SARS-CoV-2 RBD was covalently attached to paramagnetic M-270 epoxy Dynabeads using the Dynabeads Antibody Coupling Kit (catalog no. 14311D; Thermo Fisher Scientific) according to manufacturer's instructions for labeling 60 mg of beads. Beads were prepared using 30 µg of RBD per mg of beads. After coupling, beads were suspended at a concentration of 10 mg/ml in storage buffer containing 0.02% (w/v) sodium azide for up to 2 wk at 4°C. Immediately before use, RBD-coupled beads were washed once for 5 min in PBS with 0.1% BSA and then resuspended in DPBS at a concentration of 30 mg/ml. Patient sera were added to beads at a ratio of 1:10 (v/v) and gently mixed for 1 h at ambient temperature using a rotating mixer. Depleted sera were separated from beads with a magnet tube rack and transferred to a fresh tube that contained RBD-coupled beads equal in amount to the first depletion, which had been separated from the storage solution. Samples were incubated again for 1 h at ambient temperature and then magnetically separated from beads yielding RBD-depleted sera diluted 1 to 10 in DPBS. Samples were aliquoted and stored at −80°C prior to use in binding assays or neutralization assays, as described above. End-point binding titers for this assay were interpolated based on a sigmoidal four-parameter logistic, where X is concentration using 3× background as the baseline value. Neutralization titers were calculated as previously stated. Percentage reduction was then calculated from the fold change between the predepletion and postdepletion samples.

Statistics

Data were analyzed using GraphPad Prism 8.4.3. A one-way ANOVA Brown–Forsythe test or Holm–Sidak multiple t test was used as appropriate for all comparisons of cell populations and Ab titers between groups. Pearson correlation coefficients and linear regressions were applied as appropriate.

Results

Highly expanded plasmablasts and reduced MBC frequencies in peripheral blood of hospitalized COVID-19 patients

To define the dynamics of human B cell responses during acute SARS-CoV-2 infection, we assessed CD19$^+$ cell subsets in a cross-sectional study of 46 hospitalized patients, sampled at timepoints ranging from 3 to 57 d postsymptom onset (DpSO), compared with eight healthy control samples collected during the study period and confirmed to be SARS-CoV-2–negative by serology (Fig. 1). Six of the acutely infected patients were sampled at least twice (Supplemental Table I). We found that the overall B cell compartment (CD19$^+$ cells) in peripheral blood was significantly increased in the second (19.1 ± 7.54) and third (15.1 ± 6.69) weeks after symptom onset as compared with healthy controls (9.16 ± 2.67; $p < 0.001$, $p = 0.017$). This increase is likely due to both plasmablast expansion as well as a loss of peripheral CD3$^+$ T cells (Supplemental Fig. 1), as has been previously reported (26). Focusing on Ag-experienced B cell subsets, we analyzed both infection-induced plasmablasts and total MBCs. We found highly expanded plasmablast responses in the majority of COVID-19 patients, arising early after symptom (<day 7) onset (5.0 ± 1.7; $p = 0.016$), peaking at 8–14 DpSO (19.5 ± 17.6; $p < 0.001$), and remaining significantly increased 15–21 DpSO (14.5 ± 14.5; $p = 0.006$), as compared with healthy controls (1.3 ± 0.6). In contrast, classical MBCs (CD27$^+$/IgD$^-$ B cells) were significantly reduced, falling before 7 DpSO (healthy control = 23.2 ± 7.2, COVID = 9.4 ± 3.3; $p = 0.003$) and remaining low in patients at >21 d of illness (13.4 ± 5.8; $p = 0.044$). CD27$^-$ MBCs were not significantly reduced in frequency at any timepoint. Additionally, unswitched MBC (CD27$^+$/IgD$^+$) were dramatically reduced ≤7 DpSO (2.6 ± 0.9) compared with controls (14.2 ± 6.9; $p = 0.008$) and remained low in patients hospitalized >21 DpSO (3.2 ± 2.2; $p = 0.008$). Unswitched MBC are known to exhibit reactivity similar to naive B cells and are able to rapidly respond to Ag (22). The significant loss observed may be in part due to differentiation into plasmablasts, but this issue requires further study. However, both CD27$^+$- and CD27$^-$-switched MBCs remained low after 21 DpSO, when plasmablasts were no longer significantly expanded, at least in peripheral blood. These data show an early expansion of plasmablasts that is reminiscent of other serious viral infections, such as H1N1 influenza (27), dengue (28), and Ebola (29) infection, and is likely responsible for the early SARS-CoV-2–specific Ab responses seen in these patients.

RBD-specific memory B cells appear 8–14 d after symptom onset

To further assess the dynamics of B cell responses to SARS-CoV-2, we analyzed Ag-specific MBC responses by flow cytometry, using fluorescently labeled RBD as a probe (Fig. 2A). We observed a significant expansion of RBD-specific–switched MBC at 8–14 DpSO, corresponding to 0.57 ± 0.53% of the overall MBC population compared with the negligible background of 0.07 ± 0.02% in the healthy controls ($p = 0.005$) (Fig. 2B). The mean frequency of RBD-specific MBCs continued to increase 15–21 DpSO (0.63 ± 0.33%; $p = 0.004$) and then plateaued >21 DpSO (0.63 ± 0.37; $p = 0.027$). Notably, in some patients, a proportion of the RBD-specific–switched MBCs did not express CD27 (Supplemental Fig 2). In fact, overall, 31.6 ± 19.5% of the RBD$^+$ cells were CD27$^-$ and in one participant reached as high as 74%. This observation could be connected to the loss of CD27$^+$-switched MBCs, as the frequency of CD27 expression did not differ between RBD-specific and -nonspecific MBCs, or a sign that some RBD$^+$ MBCs are generated in an early extrafollicular or T-independent manner (30). Therefore, we have reported RBD specificity as a function of total switched MBCs (Fig. 2B).

The RBD$^+$ MBC in COVID-19 patients are primarily of the IgG isotype (Fig. 2C, 2D). RBD-specific IgM$^+$ MBC were only significantly expanded at 8–14 DpSO (0.08 ± 0.11) compared with healthy controls (0.005 ± 0.005; $p = 0.04$), and responses at that time were highly variable. IgA$^+$ MBCs were also only significantly expanded at 8–14 DpSO (0.15 ± 0.12) compared with healthy controls (0.01 ± 0.01; $p = 0.002$). Although a subset of patients did

Downloaded from http://www.jimmunol.org/ by guest on February 24, 2022

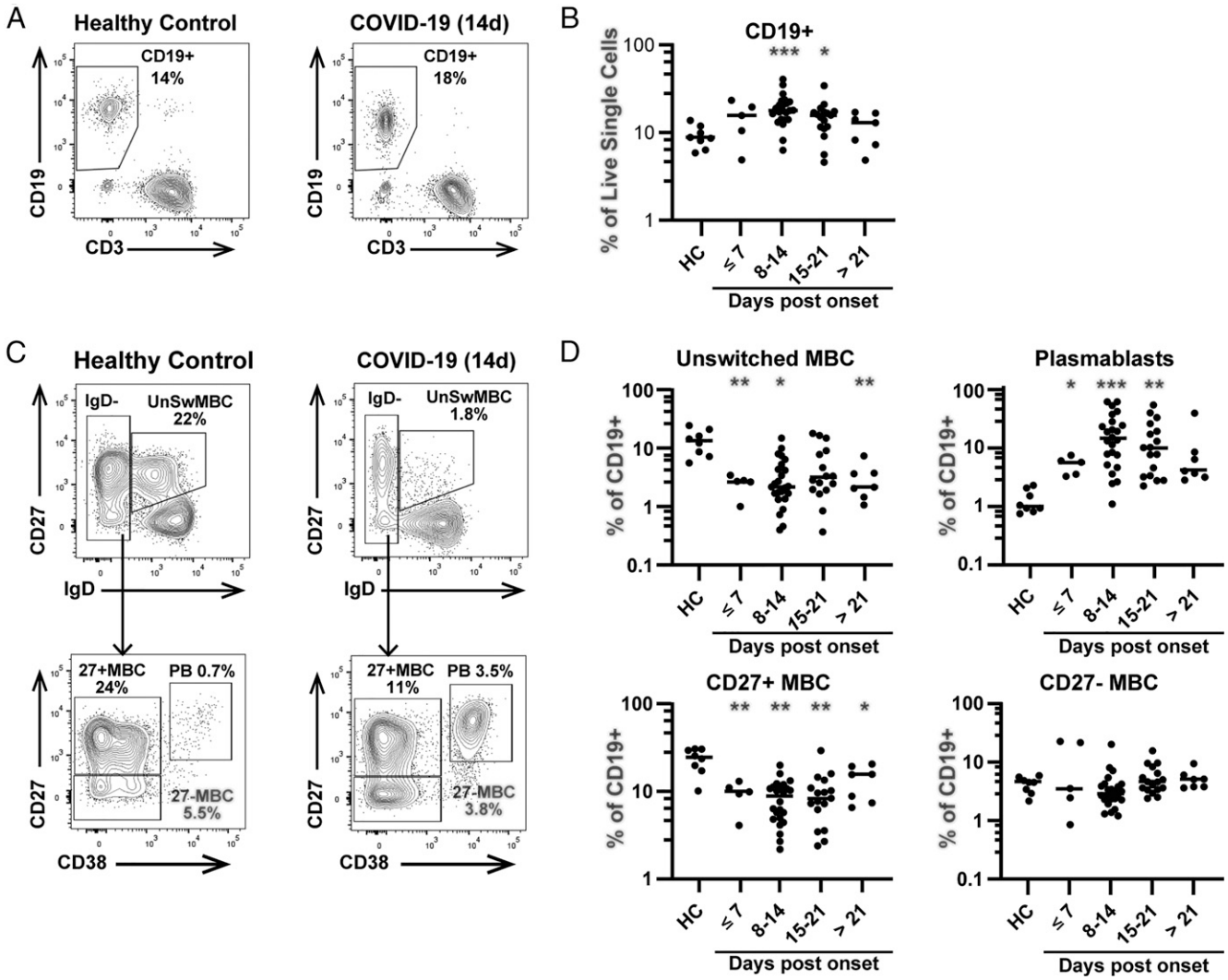

FIGURE 1. Acute COVID-19 patients exhibit loss of circulating MBCs and expansion of plasmablasts. (**A**) $CD19^+$ B cells are identified from live single $CD14^-$ $CD16^-$ cells in a healthy control (left) or COVID-19 (right) participant. (**B**) Percentage of $CD19^+$ B cells are shown for healthy controls ($n = 8$) or hospitalized COVID-19 patients ($n = 46$) over time, measured as DpSO. Six patients contributed more than one timepoint. (**C**) $CD19^+$ B cells are further subsetted as unswitched MBC, isotype-switched $CD27^+$ MBC, $CD27^-$ MBC, and plasmablasts (PB). Unswitched MBC are identified as $CD27^+$ IgD^+, and MBC and PB are IgD^- and then separated by CD27 and CD38 expression. (**D**) Unswitched MBC, $CD27^+$ MBC, $CD27^-$ MBC, and plasmablasts are shown as percentage $CD19^+$ cells in healthy controls and COVID-19 patients. Significance is calculated by Brown–Forsythe ANOVA test. $*p \leq 0.05$, $**p \leq 0.01$, $***p \leq 0.001$.

have measurable RBD^+ IgA^+ MBCs at later timepoints, other patients did not seem to mount strong IgA^+ MBC responses. In contrast, IgG^+ RBD-specific MBCs were significantly expanded starting at 8–14 DpSO (0.26 ± 0.27; $p = 0.02$) through 15–21 DpSO (0.29 ± 0.20; $p = 0.02$). By 21 DpSO or later, all donors were positive for IgG^+ RBD-specific cells (0.45 ± 0.23; $p = 0.01$) (Fig. 2D). Our data show that RBD-specific–switched MBC arise by the second week of infection and highlight that focusing on only $CD27^+$ memory may exclude a sizeable percentage of the RBD-specific memory response.

RBD-specific MBCs upregulate the activation marker CD71

Recently, activated MBC have been shown to be an important subset in several diseases, such as Ebola and influenza (29). Therefore, we assessed the expression of CD71 on the MBC of healthy controls and patients with acute SARS-CoV-2 infection and further compared the CD71 expression of non-RBD and RBD-binding MBC during disease progression (Fig. 2E, 2F). MBC obtained from healthy controls had low frequencies of $CD71^+$ (6.8 ± 1.9). In contrast, the frequency of activated switched MBCs in COVID-19 patients was significantly higher (14.3 ± 8.0; $p < 0.001$). The RBD-specific–switched MBCs express CD71 at markedly higher frequencies (42.5 ± 21.3) than non–RBD-specific MBCs. This difference was not only significant compared with healthy control MBC ($p < 0.001$) but was also significantly increased relative to non–RBD-specific MBC from the same patients ($p < 0.001$). The difference between RBD-specific and nonspecific MBC was most apparent between days 8 and 14 (RBD = 44.8 ± 16.1 versus non-RBD = 13.7 ± 7.29; $p < 0.001$) and days 14 and 21 (RBD = 27.2 ± 20.1 versus non-RBD = 17.7 ± 10.0; $p = 0.001$). These data show that not only are RBD-specific MBCs present early in the course of COVID-19, but these B cells are an active part of the ongoing immune response.

Circulating IgG and IgA titers against RBD, S, and NP Ags peak 3 wk postsymptom onset

To determine the dynamics of Ab responses during infection, we measured circulating Ab titers against SARS-CoV-2 Ags by ELISA, in the 46 individuals analyzed above, using recombinant RBD,

Downloaded from http://www.jimmunol.org/ by guest on February 24, 2022

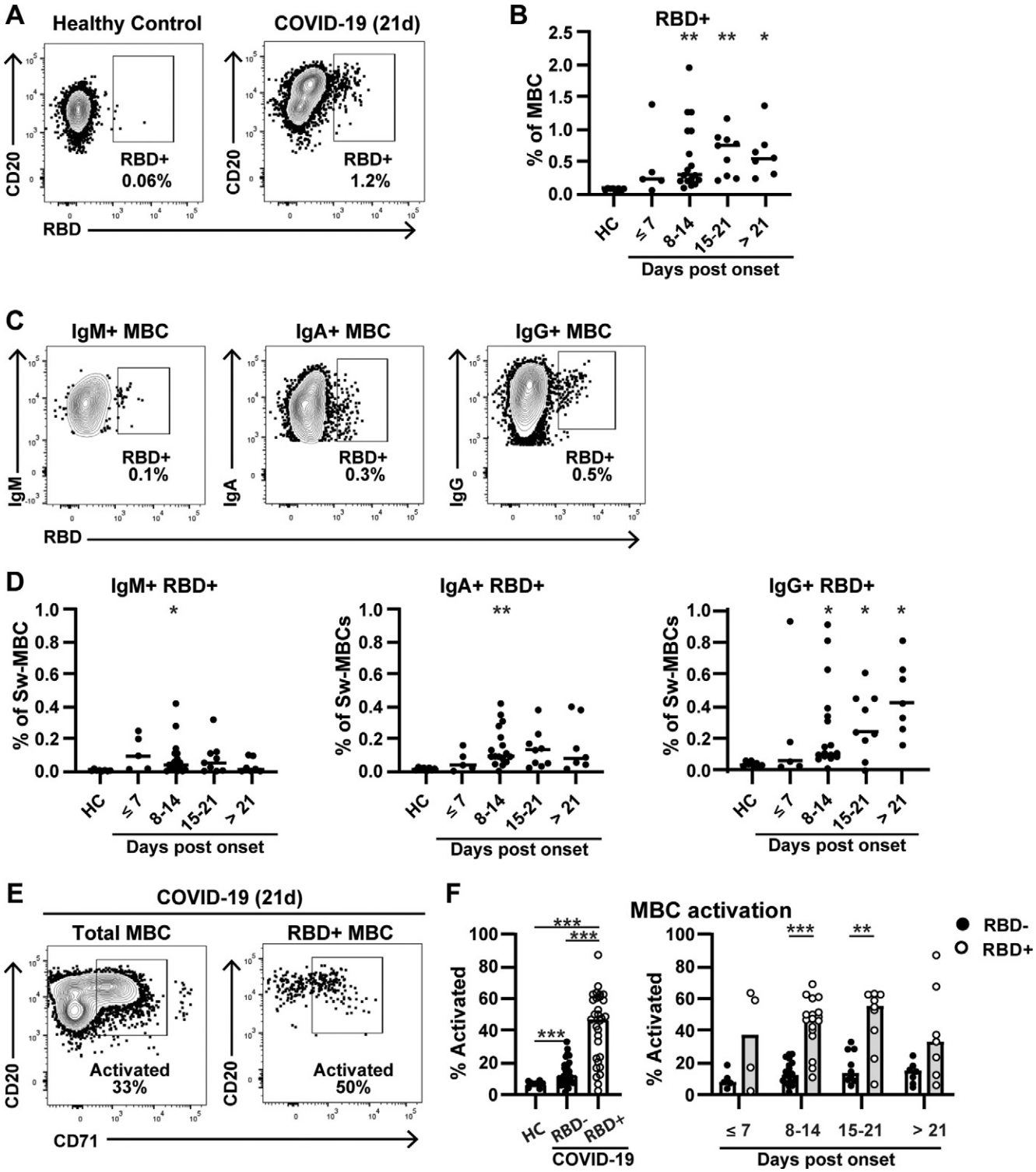

FIGURE 2. RBD-specific MBC expand rapidly and exhibit high levels of activation in COVID-19 patients. (**A**) RBD-specific MBC ($CD19^+$ $CD20^+$ IgD^- $CD38^-$) are shown for a healthy control (left) or COVID-19 patient (right). (**B**) RBD^+ MBCs are shown as a percentage of total MBCs for healthy controls ($n = 8$) and COVID-19 patients ($n = 34$) over time. Four COVID-19 patients contribute repeat timepoints. (**C**) Gating is shown for IgM^+ (left), IgA^+ (middle), and IgG^+ (right) RBD^+ MBCs in the COVID-19 patient shown in (A). Percentages shown are percentage of total MBC. (**D**) RBD^+ MBCs are shown as in (B), split into IgM^+ (left), IgA^+ (middle), and IgG^+ (right). (**E**) Activated B cells, gated by CD71 expression, for both total (left) and RBD^+ (right) MBCs. (**F**) Left, Total activation in healthy controls ($n = 8$) and COVID-19 patients RBD^- MBC ($n = 33$) or RBD^+ MBC ($n = 30$). (F) Right, A comparison of activation over time between RBD^- and RBD^+ MBCs. Significance is calculated by Brown–Forsythe ANOVA test (B, D, and F, left) or Holm–Sidak multiple *t* test (F, right). $*p \leq 0.05$, $**p \leq 0.01$, $***p \leq 0.001$.

monomeric S, or NP. In agreement with previous reports showing that seroconversion against SARS-CoV-2 and other coronaviruses occurs within 2 wk postsymptom onset (6, 9, 10), all but two individuals in the cohort had positive IgG and IgA titers against all three Ags by 2 wk postsymptom onset. IgG and IgA titers against all Ags trended with DpSO, with significant increases in Ab titer

Downloaded from http://www.jimmunol.org/ by guest on February 24, 2022

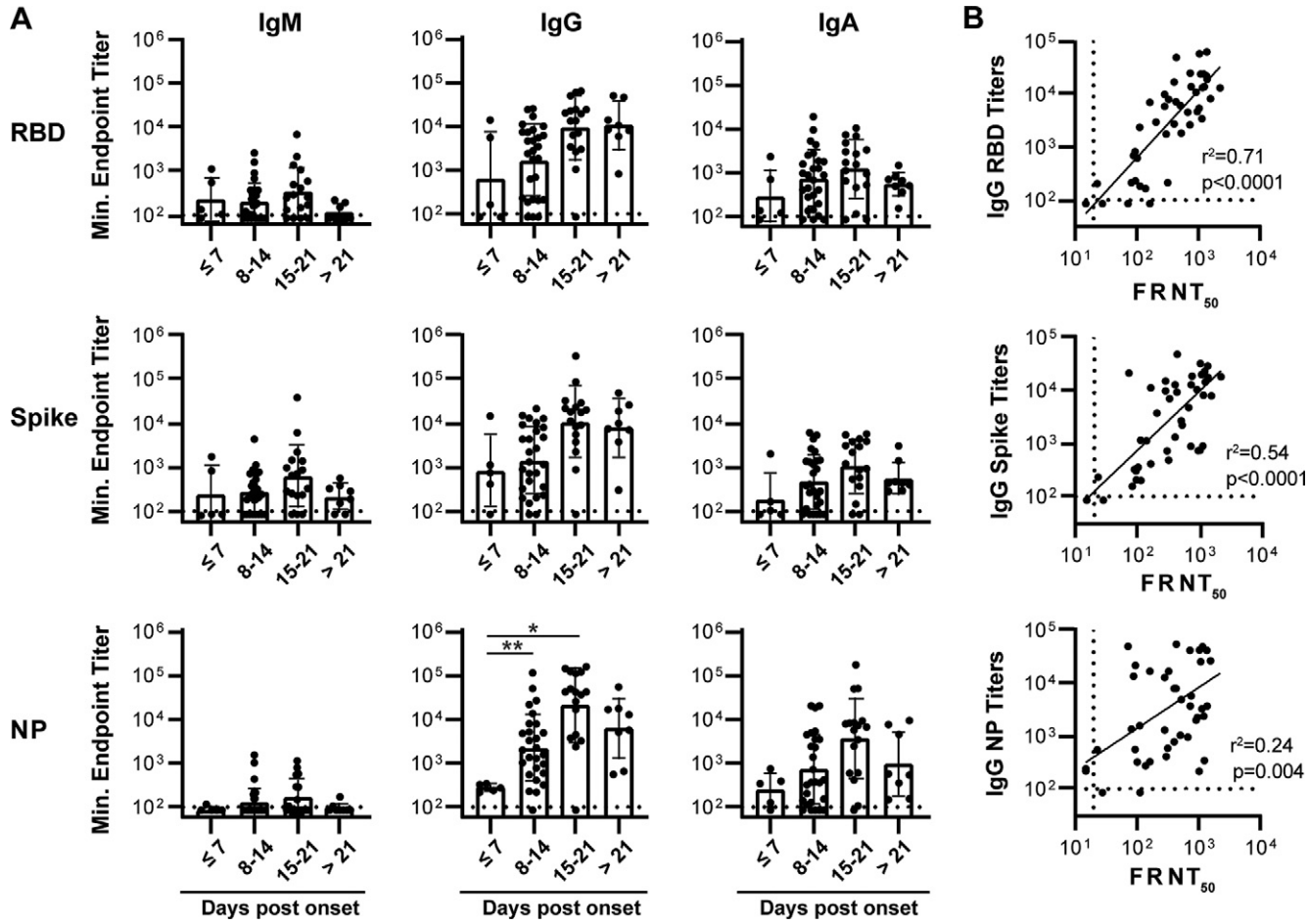

FIGURE 3. RBD-binding fraction of patient serum Ab strongly correlates with neutralization capacity. (**A**) ELISA end-point titers for serum binding against SARS-CoV-2 RBD, S, and NP recombinant protein from a cohort of acutely infected individuals (n = 46). Significance is calculated by Brown–Forsythe ANOVA test. *$p \leq 0.05$, **$p \leq 0.01$ (**B**) IgG binding titers against RBD, S, and NP correlated with SARS-CoV-2 serum neutralization activity. The coefficient of determination (r^2) is reported following linear regression analysis.

observed between the first, second, and third weeks postsymptom onset with the NP-specific IgG serum fraction (Fig. 3A). Between 8–14 DpSO, 93 (25/27), 93, (25/27), and 96% (26/27) of individuals had positive IgG titers toward RBD, S, and NP, respectively, as compared with 88 (24/27), 78 (21/27), and 81% (22/27) of individuals with positive IgA titers (Fig. 3A, Supplemental Table I). We also note that, whereas IgG titers against all Ags remain robust in individuals greater than a month postsymptom onset, IgA titers tended to decrease in the individuals sampled 1 mo postonset as compared with the early timepoints (Fig. 3A). Thus, the Ab responses to SARS-COV-2 infection were dominated by IgG, even early postinfection, illustrating that isotype switching occurs rapidly during the acute infection, with lower level responses of the IgM and IgA isotypes also detectable in most donors.

Almost all of the acutely infected hospitalized patients had detectable SARS-CoV-2–neutralizing Ab responses (Fig. 3B), with an average reciprocal titer of 568 and a range from 23 to 2205 (Supplemental Table I). These responses displayed a strong correlation with RBD-specific IgG Ab titers, as we have previously shown (Fig. 3B) (8). Although weaker than the correlation with RBD-specific IgG titers, neutralization titers also had a positive correlation with anti-S IgG titers (Fig. 3B). Finally, NP-specific IgG titers correlated quite poorly with SARS-CoV-2 neutralization (Fig. 3B). Overall, these data illustrate the occurrence of a rapid and robust Ab response to multiple SARS-CoV-2 Ags in individuals with severe COVID-19.

The RBD-specific serum fraction is responsible for neutralizing activity in a majority but not all hospitalized COVID-19 patients

As has been previously reported, circulating titers of RBD-specific IgG correlated with time after disease onset (8) (Supplemental Fig 3) and with serum-neutralizing potency (Fig. 3B). Given differences in time of sampling between patients and limited clinical data, we were unable to correlate metrics of disease severity or resolution within this cohort to RBD-specific titers (Supplemental Table I). To quantify the overall contribution of RBD-specific Abs to SARS-CoV-2 viral neutralization, we depleted RBD binding Abs from serum samples collected from a randomly selected subset of infected patients. To assess the effectiveness of the depletion, we determined the end-point RBD binding titer for paired pre- and postdepletion serum samples. We found that all samples were efficiently depleted, with an average percentage reduction of RBD-specific IgG of 98% (Fig. 4B). Irrespective of the initial titer (Fig. 4A, 4B), it is important to note that a subset of individuals had postdepletion titers that dropped below the limit of detection (Fig. 4A). For these individuals, the fold reduction was estimated by using half the limit of detection as a baseline value (10) and therefore may be greater than what was measurable in this assay. The pre- and postdepletion serum samples from each individual were then analyzed using a viral neutralization assay. Predepletion, reciprocal neutralization titers ranged from 154 to 10,270, with a median titer of 973 (Fig. 4C). Postdepletion, 13 individuals had titers above baseline, and the remaining

Downloaded from http://www.jimmunol.org/ by guest on February 24, 2022

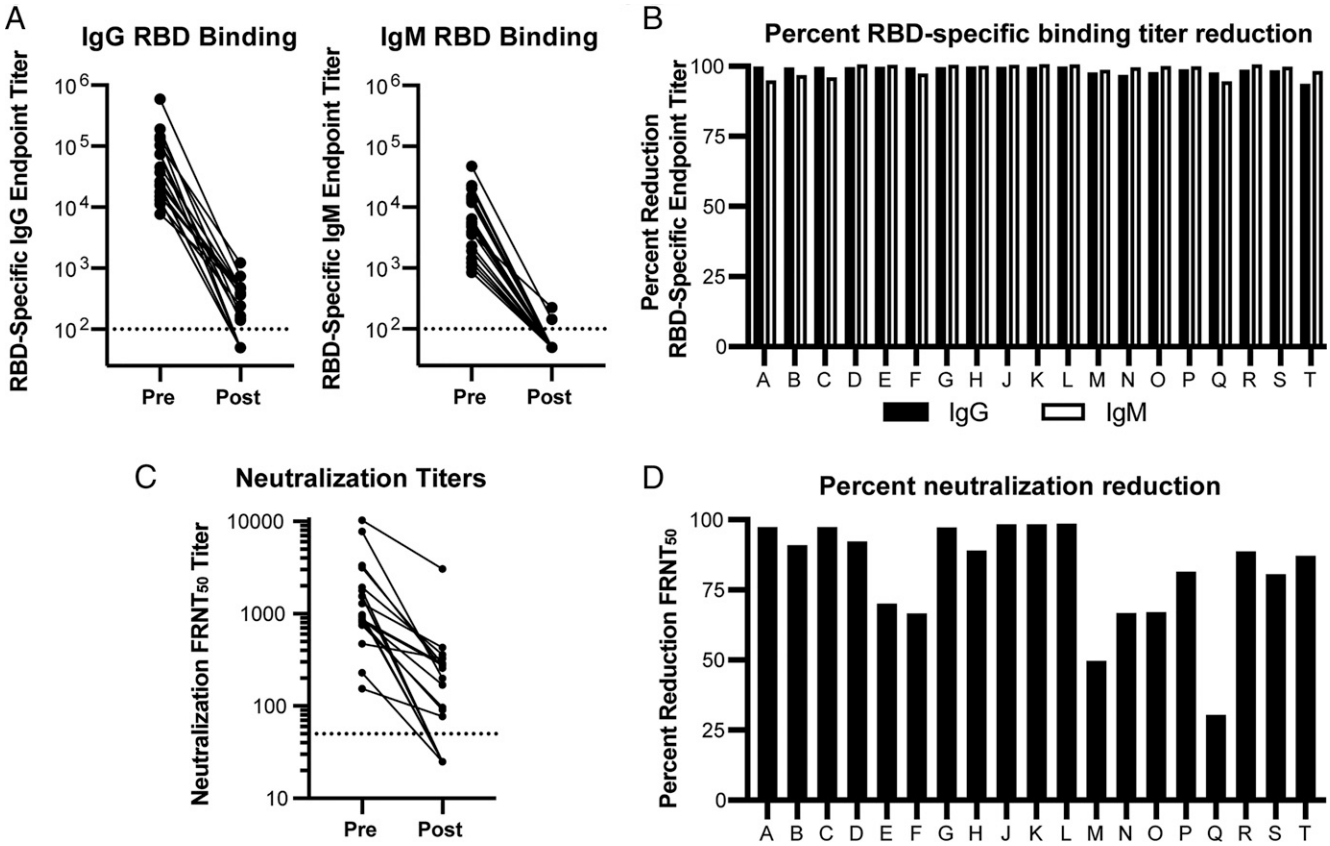

FIGURE 4. SARS-CoV-2 viral neutralization activity is mediated by RBD-specific Abs in a majority of COVID-19 patients. (**A**) ELISA end-point titers for SARS-CoV-2 RBD-specific IgG and IgM in sera from 19 acute COVID-19 patients before (Pre) and after (Post) depletion of RBD binding Abs. (**B**) For each patient, bars represent the percentage reduction in serum IgG (black) or IgM (white) RBD binding end-point titers relative to predepleted samples. (**C**) Serum neutralization activity against SARS-CoV-2 before and after depleting RBD binding Abs. Values represent the $FRNT_{50}$ titer. (**D**) For each donor, the effect of reducing RBD binding serum Abs on the viral neutralization titer is expressed as percentage reduction in the $FRNT_{50}$ value relative to predepleted samples.

individuals had titers below the limit of detection (Fig. 4C). The neutralization potency of depleted serum samples was markedly reduced in the majority of individuals assayed relative to predepletion control samples. Specifically, 13 of 19 of serum samples had a greater than 80% reduction in the viral neutralization titers as a consequence of depleting the RBD binding Abs (Fig. 4C, 4D). These results provide evidence that epitopes within the RBD are the main target of Ab-mediated viral neutralization in these individuals. In the remaining six individuals, four had >65% reduction in neutralization titer, and the remaining two individuals had 49.7 and 30.3% reductions in neutralization, respectively (Fig. 4C, 4D). This observation indicates that these donors retained more than 30% of their neutralization activity, despite RBD depletion (Fig. 4D). This result indicates that over one third of the neutralizing activity in these individuals may be due to Abs that do not bind directly to the RBD region of S or that bind to a confirmation of RBD that is not preserved in its recombinant form. Taken together, this analysis shows that, whereas the majority of neutralizing Abs are RBD specific, some individuals may generate neutralizing responses that target non-RBD epitopes. These Abs may represent an important class of Igs that could act in synergy with clinically relevant RBD-specific neutralizing Abs or enhance protection from other coronaviruses and SARS-CoV-2 RBD escape variants.

Discussion

Important components of the humoral response to viral infection include not only a rapid expansion of Ab-secreting cells to boost circulating serum titers toward the invading pathogen but also the formation of an Ag-specific MBC pool responsible for long-lasting protection. Although multiple groups have described strong B cell responses in SARS-CoV-2 patients and RBD-specific MBC encoding neutralizing Abs at convalescence, the dynamics of these responses have not been well characterized, either cross-sectionally or longitudinally. Furthermore, several recent reports (20, 21) have described "dysregulated" B cell responses during severe SARS-CoV-2 infection, suggesting mechanisms that could lead to ineffective and short-lived Ab responses, as in the case of chronic viral infections such as HIV (31) and hepatitis C virus (32). A failure to develop, or a later loss of, germinal center structures within the lymph nodes of deceased COVID-19 patients (16) and the abundance of several extrafollicular B cell populations in patients with severe COVID-19, normally observed in autoimmune individuals (such as double-negative B cells) (20), have suggested this dysregulation. In our cohort of acutely infected SARS-CoV-2 patients, we found robust infection-induced plasmablast responses and the development of RBD-specific MBCs that exhibited greater activation than their non–RBD-specific counterparts. Taken together, these data provide evidence for robust and functional humoral response to SARS-CoV-2 infection, even in the face of severe disease. However, we also observe that, within the RBD-specific MBC compartment, a significant fraction of the cells are negative for CD27, a population that has been previously described to have an extrafollicular origin (22). This finding is line with previous reports (16, 20, 21) that SARS-CoV-2 infection generates an extrafollicular response and raises questions as to the contribution of these extrafollicular subsets to the

Downloaded from http://www.jimmunol.org/ by guest on February 24, 2022

robustness and durability of the immune response against SARS-CoV-2. In addition, we observe a significant decrease of the unswitched MBC population in infected individuals, which could also be suggestive of immune dysregulation. These findings clearly highlight the heterogeneity of COVID-19 as a disease and the continued need to dissect the cellular response to SARS-CoV-2 infection.

In the case of previously studied coronaviruses, both pandemic and endemic species, seroconversion has been reported to take place within two to three weeks from the time of infection (33–35). It has now been well documented in cohorts containing both mild and severe cases of COVID-19 that, on average, seroconversion takes place two weeks postinfection (9, 10). Our serological analysis of a cohort of patients with severe COVID-19 supports the findings of previously published reports, with the majority of individuals exhibiting positive titers against multiple SARS-CoV-2 Ags by two weeks postsymptom onset. This analysis suggests that, even in individuals with severe COVID-19, the humoral response to SARS-CoV-2 remains functional. In fact, as has been previously reported (9, 11), individuals with greater disease severity tend to have higher levels of RBD binding Abs in circulation, suggesting a robust humoral response to infection. Although this trend could be potentially due to later seroconversion in these individuals (i.e., a delayed Ab response), previous studies of SARS-CoV patients demonstrate that patients with both earlier seroconversion and, in some cases, higher Ab titers were more likely to experience severe disease (36, 37). The data presented in this study support a model in which neutralizing Abs may be insufficient for mitigating disease progression and pathology in certain individuals. Critical questions remain as to why circulating Ab responses observed in our cohort were unable to prevent severe disease, given that the serum Abs were able to bind effectively to multiple viral Ags and potently neutralize the virus in vitro. Thus, the contribution and functional role of the humoral response in severe SARS-CoV-2 infection in vivo still needs to be elucidated.

We have previously reported a highly significant correlation between serum-neutralizing potency in vitro and RBD binding titers (8), as have others (9, 11). However, recent investigations into both the cellular and serological aspects of the B cell response to SARS-CoV-2 infection have begun to raise questions about the contribution of Abs derived against additional antigenic targets (17). Although the strongest correlation within our cohort is undoubtably between anti-RBD IgG titers and serum neutralization, significant correlations can also be found between full-length S and NP Ab titers and serum neutralization. Despite the significant body of evidence that now exists supporting the neutralizing potential of RBD-specific Abs (38), it is possible that Abs targeting epitopes outside of RBD could also contribute to neutralization potency. To provide quantitative evidence for the role of RBD-specific Abs in circulating serum neutralization, we employed a strategy similar to that previously published by He et al. (39) after the SARS pandemic in 2002-2003. We show that depletion of the RBD-specific serum fraction reduced the neutralizing potency of the remaining serum Ab by greater than 80% in 13 out of 19 individual serum samples tested. Interestingly, the percentage of RBD-specific B cells observed within the cohort represented an exceedingly small percentage of the overall MBC population. The contrast between the small percentage of RBD-specific MBCs observed and their potent contribution to the neutralizing activity is echoed by the findings of Rogers et al. (40), in which the percentage of RBD-specific Abs derived from S-specific MBCs was minimal, and yet, the RBD-specific Abs contributed an equal number of neutralizing Abs as their non-RBD counterparts. In addition, this group also found that the non-RBD Abs had lower neutralization than their RBD-specific counterparts and failed to provide protection in an in vivo small animal model (40). In contrast, a subset of the donors we analyzed showed a significant residual activity after RBD depletion, such that greater than 30% of the neutralization activity remained after depletion. There could be a number of explanations for this difference. It is possible that non-RBD Abs are most potent in a synergistic environment in which Abs against multiple epitopes or Ags act together to elicit neutralizing responses; this hypothesis would explain why neutralization effects observed in serum are not seen when testing mAbs. Alternatively, these donors may have initiated a response that produced potently neutralizing Abs to non-RBD epitopes. Analysis of mAbs derived from these donors is currently ongoing. In conclusion, whereas our study shows that the majority of neutralizing activity in circulating serum is driven by RBD-specific Abs, questions remain concerning the importance and combinatorial potency of non-RBD Abs in vivo. This finding has potential implications for vaccine design, as it appears that generation of Abs targeting solely SARS-CoV-2 RBD are sufficient for viral neutralization in the majority of individuals assayed. Thus, vaccines containing RBD rather than full-length S or whole virus would seem likely provide sufficient, if not greater, elicitation of SARS-CoV-2 neutralizing Abs. It was also found that a subset of individuals possess neutralizing Abs targeting potentially non-RBD epitopes, which could lead to the discovery of potent neutralization targets outside the RBD. Further investigation is necessary to ascertain the targets of the neutralizing Abs, as confirmation of RBD can be critical for the function of specific Ab subsets, and thus, we cannot confirm that these Abs do not bind to RBD in some form. Taken together, these findings serve as a platform for further exploration of the immune response to SARS-CoV-2 and will be instructive for current vaccine design and development and optimization of prophylactic and therapeutic strategies based on mAbs.

Acknowledgments

We acknowledge the contribution of the staff at both the Vaccine Research Center at Emory Children's Center and Hope Clinic for coordinating the clinical aspects of this study.

Disclosures

E.J.A. has received personal fees from AbbVie, Pfizer, and Sanofi Pasteur for consulting, and his institution receives funds to conduct clinical research unrelated to this manuscript from MedImmune, Regeneron, PaxVax, Pfizer, GSK, Merck, Novavax, Sanofi Pasteur, Janssen, and Micron. He also serves on a safety monitoring board for Kentucky BioProcessing, Inc. The other authors have no financial conflicts of interest.

References

1. Zhou, P., X. L. Yang, X. G. Wang, B. Hu, L. Zhang, W. Zhang, H. R. Si, Y. Zhu, B. Li, C. L. Huang, et al. 2020. A pneumonia outbreak associated with a new coronavirus of probable bat origin. *Nature* 579: 270–273.
2. Dong, E., H. Du, and L. Gardner. 2020. An interactive web-based dashboard to track COVID-19 in real time. *Lancet Infect. Dis.* 20: 533–534.
3. Oliver, S. E., J. W. Gargano, M. Marin, M. Wallace, K. G. Curran, M. Chamberland, N. McClung, D. Campos-Outcalt, R. L. Morgan, S. Mbaeyi, et al. 2020. The Advisory Committee on Immunization Practices' Interim Recommendation for Use of Pfizer-BioNTech COVID-19 Vaccine - United States, December 2020. *MMWR Morb. Mortal. Wkly. Rep.* 69: 1922–1924.
4. Oliver, S. E., J. W. Gargano, M. Marin, M. Wallace, K. G. Curran, M. Chamberland, N. McClung, D. Campos-Outcalt, R. L. Morgan, S. Mbaeyi, et al. 2021. The Advisory Committee on Immunization Practices' Interim Recommendation for Use of Moderna COVID-19 Vaccine - United States, December 2020. *MMWR Morb. Mortal. Wkly. Rep.* 69: 1653–1656.
5. Zhao, J., S. Zhao, J. Ou, J. Zhang, W. Lan, W. Guan, X. Wu, Y. Yan, W. Zhao, J. Wu, et al. 2020. COVID-19: coronavirus vaccine development updates. *Front. Immunol.* 11: 602256.
6. Huang, A. T., B. Garcia-Carreras, M. D. T. Hitchings, B. Yang, L. C. Katzelnick, S. M. Rattigan, B. A. Borgert, C. A. Moreno, B. D. Solomon, L. Trimmer-Smith, et al. 2020. A systematic review of antibody mediated immunity to coronaviruses:

Downloaded from http://www.jimmunol.org/ by guest on February 24, 2022

kinetics, correlates of protection, and association with severity. *Nat Commun.* 11: 4704.
7. Walls, A. C., Y. J. Park, M. A. Tortorici, A. Wall, A. T. McGuire, and D. Veesler. 2020. Structure, function, and antigenicity of the SARS-CoV-2 spike glycoprotein. [Published erratum appears in 2020 *Cell* 183: 1735. *Cell* 181: 281–292.e6.
8. Suthar, M. S., M. Zimmerman, R. Kauffman, G. Mantus, S. Linderman, A. Vanderheiden, L. Nyhoff, C. Davis, S. Adekunle, M. Affer, et al. 2020. Rapid generation of neutralizing antibody responses in COVID-19 patients. *Cell Rep. Med.* 1: 100040.
9. Graham, N. R., A. N. Whitaker, C. A. Strother, A. K. Miles, D. Grier, B. D. McElvany, E. A. Bruce, M. E. Poynter, K. K. Pierce, B. D. Kirkpatrick, et al. 2020. Kinetics and isotype assessment of antibodies targeting the spike protein receptor-binding domain of severe acute respiratory syndrome-coronavirus-2 in COVID-19 patients as a function of age, biological sex and disease severity. *Clin. Transl. Immunol.* 9: e1189.
10. Iyer, A. S., F. K. Jones, A. Nodoushani, M. Kelly, M. Becker, D. Slater, R. Mills, E. Teng, M. Kamruzzaman, W. F. Garcia-Beltran, M. Astudillo, et al. 2020. Persistence and decay of human antibody responses to the receptor binding domain of SARS-CoV-2 spike protein in COVID-19 patients. *Sci. Immunol.* 5: eabe0367.
11. Robbiani, D. F., C. Gaebler, F. Muecksch, J. C. C. Lorenzi, Z. Wang, A. Cho, M. Agudelo, C. O. Barnes, A. Gazumyan, S. Finkin, et al. 2020. Convergent antibody responses to SARS-CoV-2 in convalescent individuals. *Nature* 584: 437–442.
12. Du, L., Y. He, Y. Zhou, S. Liu, B. J. Zheng, and S. Jiang. 2009. The spike protein of SARS-CoV–a target for vaccine and therapeutic development. *Nat. Rev. Microbiol.* 7: 226–236.
13. Kreer, C., M. Zehner, T. Weber, M. S. Ercanoglu, L. Gieselmann, C. Rohde, S. Halwe, M. Korenkov, P. Schommers, K. Vanshylla, et al. 2020. Longitudinal isolation of potent near-germline SARS-CoV-2-neutralizing antibodies from COVID-19 patients. [Published erratum appears in 2020 *Cell* 182: 1663–1673.] *Cell* 182: 843–854.e12.
14. Wan, J., S. Xing, L. Ding, Y. Wang, C. Gu, Y. Wu, B. Rong, C. Li, S. Wang, K. Chen, et al. 2020. Human-IgG-neutralizing monoclonal antibodies block the SARS-CoV-2 Infection. *Cell Rep.* 32: 107918.
15. Zost, S. J., P. Gilchuk, J. B. Case, E. Binshtein, R. E. Chen, J. P. Nkolola, A. Schäfer, J. X. Reidy, A. Trivette, R. S. Nargi, et al. 2020. Potently neutralizing and protective human antibodies against SARS-CoV-2. *Nature* 584: 443–449.
16. Kaneko, N., H. H. Kuo, J. Boucau, J. R. Farmer, H. Allard-Chamard, V. S. Mahajan, A. Piechocka-Trocha, K. Lefteri, M. Osborn, J. Bals, et al. 2020. The loss of Bcl-6 expressing T follicular helper cells and the absence of germinal centers in COVID-19. *SSRN*, 3652322.
17. Juno, J. A., H. X. Tan, W. S. Lee, A. Reynaldi, H. G. Kelly, K. Wragg, R. Esterbauer, H. E. Kent, C. J. Batten, F. L. Mordant, et al. 2020. Humoral and circulating follicular helper T cell responses in recovered patients with COVID-19. *Nat. Med.* 26: 1428–1434.
18. He, Z., Q. Dong, H. Zhuang, S. Song, G. Peng, G. Luo, and D. E. Dwyer. 2004. Kinetics of severe acute respiratory syndrome (SARS) coronavirus-specific antibodies in 271 laboratory-confirmed cases of SARS. *Clin. Diagn. Lab. Immunol.* 11: 792–794.
19. Wang, F., J. Nie, H. Wang, Q. Zhao, Y. Xiong, L. Deng, S. Song, Z. Ma, P. Mo, and Y. Zhang. 2020. Characteristics of peripheral lymphocyte subset alteration in COVID-19 pneumonia. *J. Infect. Dis.* 221: 1762–1769.
20. Woodruff, M. C., R. P. Ramonell, D. C. Nguyen, K. S. Cashman, A. S. Saini, N. S. Haddad, A. M. Ley, S. Kyu, J. C. Howell, T. Ozturk, et al. 2020. Extrafollicular B cell responses correlate with neutralizing antibodies and morbidity in COVID-19. *Nat. Immunol.* 21: 1506–1516.
21. Oliviero, B., S. Varchetta, D. Mele, S. Mantovani, A. Cerino, C. G. Perotti, S. Ludovisi, and M. U. Mondelli. 2020. Expansion of atypical memory B cells is a prominent feature of COVID-19. *Cell. Mol. Immunol.* 17: 1101–1103.
22. Taylor, J. J., K. A. Pape, and M. K. Jenkins. 2012. A germinal center-independent pathway generates unswitched memory B cells early in the primary response. *J. Exp. Med.* 209: 597–606.
23. Bentivegna, E., A. Sentimentale, M. Luciani, M. L. Speranza, L. Guerritore, and P. Martelletti. 2021. New IgM seroconversion and positive RT-PCR test after exposure to the virus in recovered COVID-19 patient. *J. Med. Virol.* 93: 97–98.
24. To, K. K., I. F. Hung, J. D. Ip, A. W. Chu, W. M. Chan, A. R. Tam, C. H. Fong, S. Yuan, H. W. Tsoi, A. C. Ng, et al. 2020. COVID-19 re-infection by a phylogenetically distinct SARS-coronavirus-2 strain confirmed by whole genome sequencing. *Clin. Infect. Dis.* ciaa1275.
25. Xie, X., A. Muruato, K. G. Lokugamage, K. Narayanan, X. Zhang, J. Zou, J. Liu, C. Schindewolf, N. E. Bopp, P. V. Aguilar, et al. 2020. An infectious cDNA clone of SARS-CoV-2. *Cell Host Microbe* 27: 841–848.e3.
26. Lucas, C., P. Wong, J. Klein, T. B. R. Castro, J. Silva, M. Sundaram, M. K. Ellingson, T. Mao, J. E. Oh, B. Israelow, et al. Yale IMPACT Team. 2020. Longitudinal analyses reveal immunological misfiring in severe COVID-19. *Nature* 584: 463–469.
27. Wrammert, J., K. Smith, J. Miller, W. A. Langley, K. Kokko, C. Larsen, N. Y. Zheng, I. Mays, L. Garman, C. Helms, et al. 2008. Rapid cloning of high-affinity human monoclonal antibodies against influenza virus. *Nature* 453: 667–671.
28. Wrammert, J., N. Onlamoon, R. S. Akondy, G. C. Perng, K. Polsrila, A. Chandele, M. Kwissa, B. Pulendran, P. C. Wilson, O. Wittawatmongkol, et al. 2012. Rapid and massive virus-specific plasmablast responses during acute dengue virus infection in humans. *J. Virol.* 86: 2911–2918.
29. Ellebedy, A. H., K. J. Jackson, H. T. Kissick, H. I. Nakaya, C. W. Davis, K. M. Roskin, A. K. McElroy, C. M. Oshansky, R. Elbein, S. Thomas, et al. 2016. Defining antigen-specific plasmablast and memory B cell subsets in human blood after viral infection or vaccination. *Nat. Immunol.* 17: 1226–1234.
30. Sanz, I., C. Wei, S. A. Jenks, K. S. Cashman, C. Tipton, M. C. Woodruff, J. Hom, and F. E. Lee. 2019. Challenges and opportunities for consistent classification of human B cell and plasma cell populations. *Front. Immunol.* 10: 2458.
31. Moir, S., J. Ho, A. Malaspina, W. Wang, A. C. DiPoto, M. A. O'Shea, G. Roby, S. Kottilil, J. Arthos, M. A. Proschan, et al. 2008. Evidence for HIV-associated B cell exhaustion in a dysfunctional memory B cell compartment in HIV-infected viremic individuals. *J. Exp. Med.* 205: 1797–1805.
32. Doi, H., S. Tanoue, and D. E. Kaplan. 2014. Peripheral CD27-CD21- B-cells represent an exhausted lymphocyte population in hepatitis C cirrhosis. *Clin. Immunol.* 150: 184–191.
33. Callow, K. A., H. F. Parry, M. Sergeant, and D. A. Tyrrell. 1990. The time course of the immune response to experimental coronavirus infection of man. *Epidemiol. Infect.* 105: 435–446.
34. Hsueh, P. R., L. M. Huang, P. J. Chen, C. L. Kao, and P. C. Yang. 2004. Chronological evolution of IgM, IgA, IgG and neutralisation antibodies after infection with SARS-associated coronavirus. *Clin. Microbiol. Infect.* 10: 1062–1066.
35. Ko, J. H., M. A. Müller, H. Seok, G. E. Park, J. Y. Lee, S. Y. Cho, Y. E. Ha, J. Y. Baek, S. H. Kim, J. M. Kang, et al. 2017. Serologic responses of 42 MERS-coronavirus-infected patients according to the disease severity. *Diagn. Microbiol. Infect. Dis.* 89: 106–111.
36. Lee, N., P. K. Chan, M. Ip, E. Wong, J. Ho, C. Ho, C. S. Cockram, and D. S. Hui. 2006. Anti-SARS-CoV IgG response in relation to disease severity of severe acute respiratory syndrome. *J. Clin. Virol.* 35: 179–184.
37. Zhang, L., F. Zhang, W. Yu, T. He, J. Yu, C. E. Yi, L. Ba, W. Li, M. Farzan, Z. Chen, et al. 2006. Antibody responses against SARS coronavirus are correlated with disease outcome of infected individuals. *J. Med. Virol.* 78: 1–8.
38. Ju, B., Q. Zhang, J. Ge, R. Wang, J. Sun, X. Ge, J. Yu, S. Shan, B. Zhou, S. Song, et al. 2020. Human neutralizing antibodies elicited by SARS-CoV-2 infection. *Nature* 584: 115–119.
39. He, Y., Q. Zhu, S. Liu, Y. Zhou, B. Yang, J. Li, and S. Jiang. 2005. Identification of a critical neutralization determinant of severe acute respiratory syndrome (SARS)-associated coronavirus: importance for designing SARS vaccines. *Virology* 334: 74–82.
40. Rogers, T. F., F. Zhao, D. Huang, N. Beutler, A. Burns, W. T. He, O. Limbo, C. Smith, G. Song, J. Woehl, et al. 2020. Isolation of potent SARS-CoV-2 neutralizing antibodies and protection from disease in a small animal model. *Science* 369: 956–963.

Downloaded from http://www.jimmunol.org/ by guest on February 24, 2022